



ISTITUTO NAZIONALE DI RICERCA METROLOGICA Repository Istituzionale

Dithiols as Liquid Crystalline Building Blocks for Smart Polymers via Thiol-yne Click Chemistry

This is the author's accepted version of the contribution published as:

Original

Dithiols as Liquid Crystalline Building Blocks for Smart Polymers via Thiol-yne Click Chemistry / Lupi, Flavia; Martella, Daniele; Nocentini, Sara; Antonioli, Diego; Laus, Michele; Wiersma, Diederik S.; Parmeggiani, Camilla. - In: ACS APPLIED POLYMER MATERIALS. - ISSN 2637-6105. - 3:3(2021), pp. 1602-1609. [10.1021/acsapm.0c01423]

Availability:

This version is available at: 11696/73324 since: 2023-05-23T08:13:38Z

Publisher:

AMER CHEMICAL SOC

Published

DOI:10.1021/acsapm.0c01423

Terms of use:

This article is made available under terms and conditions as specified in the corresponding bibliographic description in the repository

Publisher copyright

American Chemical Society (ACS)

Copyright © American Chemical Society after peer review and after technical editing by the publisher. To access the final edited and published work see the DOI above.

(Article begins on next page)

Dithiols as liquid crystalline building blocks for smart polymers via thiol-yne click chemistry

Flavia Lupi,^{1,2} Daniele Martella,^{2,3*} Sara Nocentini,^{2,3} Diego Antonioli,⁴ Michele Laus,⁴ Diederik S. Wiersma,^{2,3,5} Camilla Parmeggiani.^{2,3,6*}

1 Istituto Nazionale di Ottica (CNR-INO), Sesto Fiorentino 50019, Italy.

2 European Laboratory for Non-Linear Spectroscopy (LENS), Sesto Fiorentino 50019, Italy.

3 Istituto Nazionale di Ricerca Metrologica (INRiM), Torino 10135, Italy.

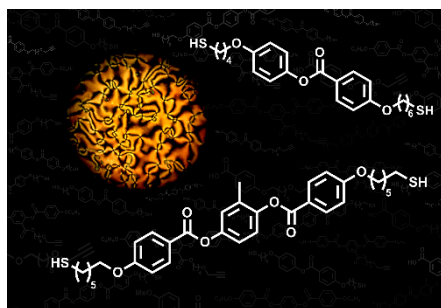
4 Dipartimento di Scienze e Innovazione Tecnologica (DISIT), Università del Piemonte Orientale "A. Avogadro", Alessandria 15121, Italy.

5 Physics and Astronomy Department, University of Florence, Sesto Fiorentino 50019, Italy.

6 Dipartimento di Chimica "Ugo Schiff", University of Florence, Sesto Fiorentino 50019, Italy.

KEYWORDS: Thiol-yne Click Chemistry, Liquid Crystalline Elastomers, Liquid Crystalline Thiols, Smart Materials, Thermoresponsive Polymers

ABSTRACT: Since 30 years, LCEs are attracting the attention of many researchers thanks to their anisotropic molecular structure which allows them to build up artificial muscles. Possible applications span from soft robotics to biomedical or tunable optical devices. The power of thiol-yne click chemistry was recently demonstrated in the preparation of smart polymers, in particular Liquid Crystalline Elastomers (LCEs), in which the mesogenic units are incorporated both in the main-chain and as pendant groups. To enrich the library of available LCE materials, in this work, several liquid crystalline dithiols and alkynes have been synthesized and copolymerized to obtain elastomers with different thermomechanical properties. The architecture of the main-chain was found to play a prominent role in modulating the clearing point in a range of 60 °C whereas only a minor contribution is given by the mesogens in the side-chain. On the other hand, the mechanical response resulted highly sensitive to fine details of the side-chain structure. Accordingly, the present study not only improves the basic understanding of the chemical-physical properties of LCEs, but paves the way to the preparation of multicomponent actuators able to deform in different temperature ranges, thus ultimately leading to complex soft robotic operations.



1. INTRODUCTION

Liquid Crystalline Elastomers (LCEs) are smart polymers having many potential applications thanks to their anisotropic molecular structures which can be controlled during the preparation steps.¹ The Liquid Crystalline (LC) nature confers to this class of materials several peculiar properties in comparison to standard elastomers. One example is their anisotropic mechanical response allowing for high deformation at low stress in the direction perpendicular to the LC director thanks to their soft elastic behavior.² In this case, local control over the LC alignment (for instance via patterning) can be adopted to embed stress inside specific material parts, which is useful in the realization of stretchable electronic devices.³ Furthermore, thanks to

the liquid crystalline alignment, such materials are able to efficiently dissipate energy upon shock⁴ and therefore they can be used to prepare highly dissipative elements that mimic the damping properties of biological tissues.⁵

One of the most important properties of LCEs is their responsiveness to the environment. Different types of stimuli – from temperature to light or magnetic⁶ and electric fields⁷ – can induce a modification of the LC alignment with a consequent macroscopic shape deformation.^{8, 9} When the material changes the molecular alignment, the system undergoes a contraction along the alignment direction and an expansion in the perpendicular plane. This deformation is totally reversible allowing materials to sequentially contract and relax back mimicking the behavior of muscles.¹⁰ By optimizing the material composition, synthetic smart polymers can produce forces comparable to those produced by natural muscles (up to 400 mN/mm²) and the kinetics by which the forces develop can be brought down into the millisecond regime.¹¹

All these chemical-physical properties arise from their molecular structure which is composed of two fundamental ingredients: the former is a standard liquid crystalline unit, incorporated inside the polymer, and the latter is the presence of a cross-linking agent. The synthetic strategies to prepare LCEs involve different reactions,¹² but most of them are based on the use of mesogenic acrylate monomers.¹³ These molecules can be aligned in the nematic phase and then polymerized to obtain the final material having a side-chain architecture (liquid crystal units attached as pendant groups to the polymer chain). To obtain a larger anisotropy of the polymeric backbone, that do enhance the mechanical deformation of the polymer under stimuli, several techniques have been recently developed starting from LC diacrylates to obtain main-chain architectures (liquid crystal units attached along the polymer backbone).¹⁴ These molecules can be firstly oligomerized with a dithiol by a base catalyzed Michael addition, and then crosslinked by a radical reaction.¹⁵ This two-step procedure requires the alignment of the polydomain oligomers before the crosslinking which can be achieved by mechanical stretching or extrusion in a 3D printer.¹⁶ A more recent example employs the LC diacrylates and dithiols in a direct free radical polymerization.¹⁷ In this process, radical mediated thiol-ene click reaction allows for the formation of main-chain oligomers, while the acrylate polymerization forms the crosslinked network.¹⁸

Currently, most of the examples of LCEs are based on the incorporation of the mesogenic units in the side-chain or in the main-chain while simultaneous presence in both positions is barely explored. In this direction, some of us developed a methodology to obtain polymers with a mixed side-chain, main-chain architecture in one-step by exploiting the thiol-yne click chemistry.¹⁹ Such reaction is commonly used for material functionalization or polymer crosslinking and proceeds with the attack of two thiol units to the same alkyne.²⁰ In radical condition, the thiyl radical is first produced and it promptly reacts with the alkyne to form a vinylthioether intermediate (with formation of a new thiyl radical). This species is more reactive towards thiols than the initial alkyne and then a 1,2-dithioether compound is preferentially formed.²¹

The application of thiol-yne click chemistry in the LCE field required the preparation of liquid crystalline monomers bearing thiol and alkyne moieties to obtain polymers with alternated side-chain and main-chain mesogens in the final materials. Potentially, this reaction would result in a powerful and broad synthetic tool for three reasons: i) the reaction is not oxygen-sensitive conversely to standard free radical polymerizations, thus leading to an easier material manipulation; ii) it is possible to integrate the synthetic process with different lithographic setups already employed with LCEs such as Direct Laser Writing²² or Soft Lithography;²³ iii) the polymer polymorphism can be modulated, as observed for linear systems, combining main-chain and side-chain LCs in the same backbone.²⁴

In this paper, we present new monomers and the related polymers obtained by thiol-yne click chemistry. The influence of the different units and their position in the side-chain or in the main-chain of the polymer is described. We will demonstrate that distinct properties can be independently added on the material thus leading to smart materials having properties “on request”.

2. MATERIALS AND METHODS

General methods. Monomers T1, A3 and crosslinker (Figure S1) were prepared as previously described.¹⁹ The synthesis of monomers T2, A1 and A2 is reported in Supporting Information (Schemes S1 and S2) together with their ¹H and ¹³C NMR spectra (Figures S2-7). IR spectra were recorded with a BX FTIR Perkin-Elmer system spectrophotometer. Thermal transitions were measured using a DSC TA Instruments Q-2000 calorimeter under a nitrogen atmosphere (heating and cooling rate: 10 °C/min). Polarized optical microscopy (POM) was performed using an inverted microscope (Zeiss, Axio Observer A1) with cross polarizers equipped with a Linkam PE120 hot stage. Material contractions were evaluated from optical images during a controlled heating protocol on a hot stage. Dynamic-mechanical thermal analysis (DMTA) were carried out using a DMTA V analyzer (Rheometric Scientific) in tensile mode. The measurements were performed both in the parallel and perpendicular direction with respect to the liquid crystalline alignment as a function of temperature. A scanning rate of 4 °C/min was chosen. The glass transition temperature in DMTA experiments was taken as the maximum of tan δ peaks. The analyzer is equipped with rectangular tension geometry. Specimens with size of 20 × 5 × 0.02 mm³ were employed. A strain amplitude of 0.1% (linear viscoelastic range) and a strain frequency of 1 Hz were chosen.

LCE fabrication. Monomeric mixtures were prepared by mixing a dithiol (T1 or T2, 60% mol/mol), an alkyne (A1 or A2 or A3, 20% mol/mol), the crosslinker (20% mol/mol), and the UV photoinitiator (Irgacure 369, 4% w/w of the whole mixture). The mixtures were melted in the isotropic phase and infiltrated by capillary force in a liquid crystalline cell composed by two treated glasses with a 75 μm spacer (Mylar film). The glasses were previously spin-coated with PVA solution (1% in water) and then rubbed unidirectionally with a velvet cloth. After infiltration, the cell was cooled down (2 °C/min) until formation of a homogeneous planar alignment and then irradiated for 1 hour with a UV lamp (ThorLabs M385CP1-C4, λ = 385 nm). After an additional irradiation for 30 minutes at 100 °C, cells were immersed in water to facilitate the detachment of the glass by the film, which was mechanically removed by the support using a razor blade.

3. RESULTS AND DISCUSSION

Thiol-yne click chemistry involves the radical reaction of two thiol groups with an alkyne to form a 1,2-disubstituted product. Using this process for the formation of a polymeric structure needs the reaction of a dithiol with an alkyne (chain growth), while the network formation requires also the presence of a crosslinker that can be a multifunctional thiol or alkyne. Following our previous study¹⁹, we prepared different LCEs by photopolymerization of a mixture of two mesogenic monomers, one containing two thiol groups at the end of the flexible spacers and the other functionalized by a propargylic moiety. The reaction scheme is shown in Figure 1a, also reporting the general architecture of the final polymer. In all cases, the used crosslinker is a dialkyne whose structure is reported in Figure S1. Modification of this compound has been already studied demonstrating only a small effect on the LCE properties¹⁹ and, more important, without any relevant effect on the clearing temperature of the material. In this study, the structure and amount of crosslinker has been fixed to better elucidate the role of the mesogenic units in the main-chain or in the side-chain of the polymers. Both these units have been changed exploring different LC cores. For the dithiols, we chose two different monomers (T1 and T2, Figure 1b) having different number of aromatic rings in the central core, while for the alkynes (A1, A2 and A3, Figure 1b), we modify both the number of aromatic rings, and the bonding (end-on or side-on) of the pendant group (A1 and A2 are “end-on” monomer, while A3 is a “side-on” one).

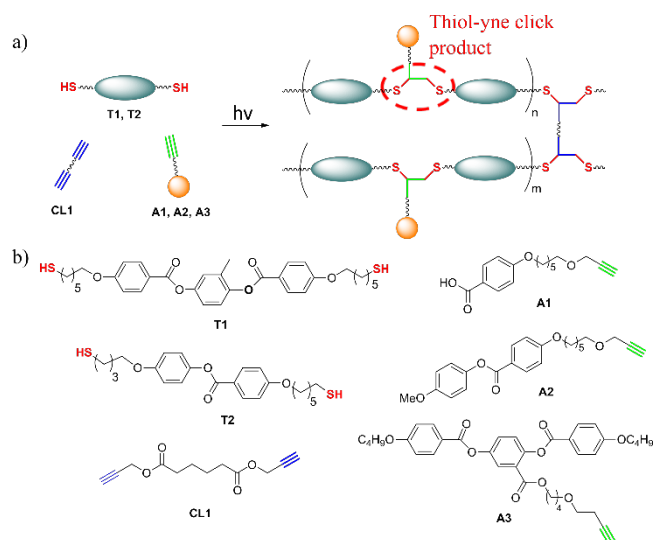


Figure 1. Monomers used for LCE preparation by thiol-yne click chemistry. a) general scheme of the synthetic methods; b) molecular structure of the liquid crystalline dithiols (on the left) and alkynes (on the right) employed in the present study.

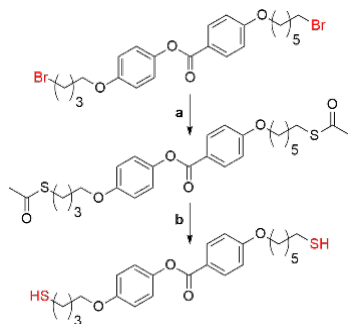


Figure 2. Key steps for the dithiol synthesis. Reagent and conditions: a) KSAc, DMF, rt, 2.5 h, 88%; b) NaBH₄, THF:H₂O 1:5, rt, 24 h, 67%.

T1 and A3 were already employed for the preparation of LCEs, while for the other new compounds, a detailed synthesis is reported in Supporting Information (Schemes S1 and S2). We highlight here how the most critical step for the monomer synthesis is the introduction of the terminal thiols. These groups were inserted in the last step (to avoid undesired side reactions during the whole process, e.g. thiol oxidation) with the two-step procedure reported in Figure 2. Starting from the corresponding LC dibromide, we first introduced the thioacetal group by reaction with potassium thioacetate and then a selective reduction by sodium borohydride was performed to obtain the desired monomer²⁵ with a 59% yield over the two steps. The variation of the monomer molecular structure leads to effective modifications of the LC properties as summarized in Table 1. The mesomorphic properties of all molecules have been studied by DSC and POM analysis (traces and POM images are reported in Supporting Information, Figures S8 and S9).

Table 1 – Thermal properties of the monomers obtained during the second heating (h) - cooling (c) cycle of DSC experiments.

Mono- mer	Phase transition temperatures [°C] ^a
T1^b	h: Cr 81 N 163 (2.1) I c: I 161 (2.1) N 45 Cr
T2	h: Cr 62 N 77 (0.56) I

	c: I 76 (0.57) N 50 LC 17 Cr
A1	h: Cr 102 N 110 (1.82) I c: I 110 (2.62) N 89 (1.86) SmA 48 Cr
A2	h: Cr 67 I c: I 48 Cr
A3^b	h: Cr 71 N 88 (1.01) I c: I 86 (1.08) N ^c

^a Determined from the onset of the transition peak. In brackets is reported the enthalpy of the transition (kJ/mol) determined from the integration of peak. ^b Data reported from literature¹⁹; ^c Crystallization was not observed on cooling until -50 °C.

Regarding the thiols, both T1 and T2 present an enantiotropic nematic phase. In T1, the extended aromatic core increases the melting temperature and broadens the nematic temperature range. T2 also presents a monotropic SmA phase on cooling which can be recognized by a typical fan-shaped texture by POM (Figure S9). For the other compounds, the alkynes A1 and A3 present LC properties while A2 does not form any mesophase.²⁶ A1 forms LCs thanks to the ability of hydrogen bonding in between carboxylic groups, and thus forming a central core by supramolecular interaction. It shows the highest melting temperature of the series and, on cooling, forms also a SmA phase. On the other hand, A3 presents LC properties also at room temperature at which crystallization did not occur even after hours. Such behavior is of fundamental importance for LCE polymerization processes at room temperature, that is highly desirable for patterning the material with common lithographic and 3D printing technologies.²⁷

The monomeric mixture has been prepared by fixing the crosslinker content (20% mol/mol, according to our previous study) and calculating the amount of the other liquid crystals following the stoichiometry of the reaction (two thiols react with one alkyne). Mixtures and their resulting polymers are noted here as LCE*a-b* where *a* is the number associated to the used thiol (1 for T1 and 2 for T2) and *b* indicate the used alkyne (1 for A1, 2 for A2 and 3 for A3).

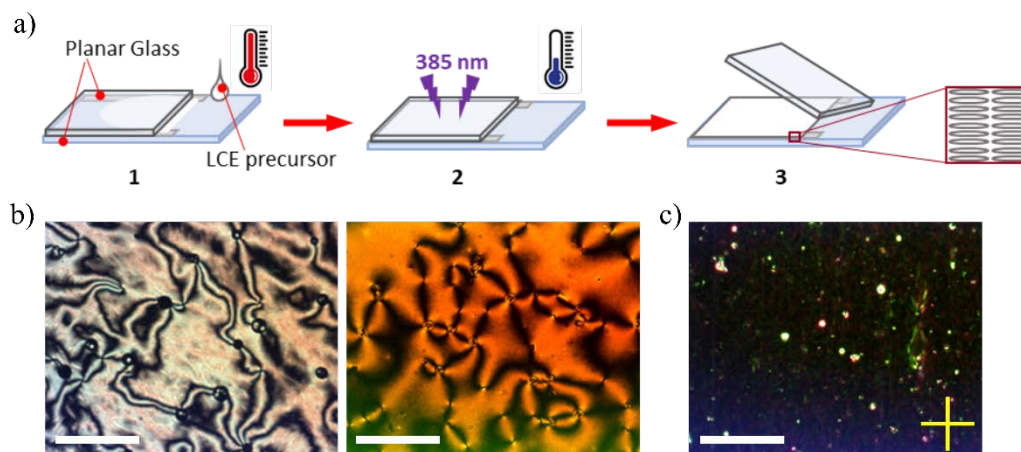


Figure 3- Material fabrication. a) Scheme of the procedure: 1 - infiltration of the melted LCE precursor into the LC cell, 2 - cooling and polymerization with a UV lamp after alignment of nematic phase, 3 - removal of the film from the cell; b) POM images (from left to right) of the nematic phase for mixture LCE1-3 and LCE2-3 between two standard glasses; c) POM image of LCE2-3 after the alignment procedure (with nematic director parallel to the polarizer transmission axis). Polarizer direction is marked in yellow. Scale bars: 200 μm .

We focused our attention on four formulations mixing T1 with the three different alkynes, and mixing T2 with A3. The other molecular combinations were not considered as the monomeric mixture composed by T2 and A2 does not present liquid crystalline behavior, while the mixture containing T2 and A1 has such a high viscosity that could not be aligned by liquid crystalline cells. All the other mixtures present only the nematic phase and do not crystallize at room temperature. Their mesomorphic properties were studied by POM and are summarized in table S1. Exemplificative pictures of the liquid crystalline phase are reported in Figure 3b where typical Schlieren nematic textures (with 2-point and 4-point defects) are detected during observation of the molecules in between two standard glasses.

The LCEs were then prepared with the well-established procedure used also for acrylate based LCEs¹³ and depicted in Figure 3a. First, the monomer mixture was melted in the isotropic phase and infiltrated by capillarity in a liquid crystalline cell. Then the cell was cooled down into the nematic phase to reach the desired alignment. After polymerization with a UV lamp, the cell was opened and the LCE detached from the glass. All films present a homogeneous planar alignment, obtained by the use of LC cells prepared from two PVA coated and rubbed glasses. The film alignment was induced by thermal annealing in the nematic phase, which cause the molecular director orientation along the rubbing direction, and checked by POM where transmittance extinction was detected for director parallel to one of the polarizer (Figure 3c). The successful polymerization can be verified by comparison of the FT-IR spectra of the unpolymerized mixture and with those of the final material (reported in Figure S10) showing the disappearance of the peak related to the C-H stretching of the terminal alkyne (3288 cm^{-1}).

The thermal properties of the LCEs were first analyzed by DSC and the relevant traces are reported in Figures 4 and S11. For all polymers, the glass and the nematic to isotropic phase transitions were observed. The glass transition temperatures (T_g) and the clearing (T_{NI}) are reported in Table 2. Changing the number of the aromatic rings inside the core of the main-chain component (T1 and T2) leads to an abrupt change of the clearing temperature which was reduced from $147\text{ }^{\circ}\text{C}$ (for LCE1-3) to $84\text{ }^{\circ}\text{C}$ (for LCE2-3). On the other hand, a minor effect of the alkyne nature was observed with a very small modulation of T_{NI} (differences in a range of about $4\text{ }^{\circ}\text{C}$ for the samples LCE1-1, LCE1-2, and LCE1-3).

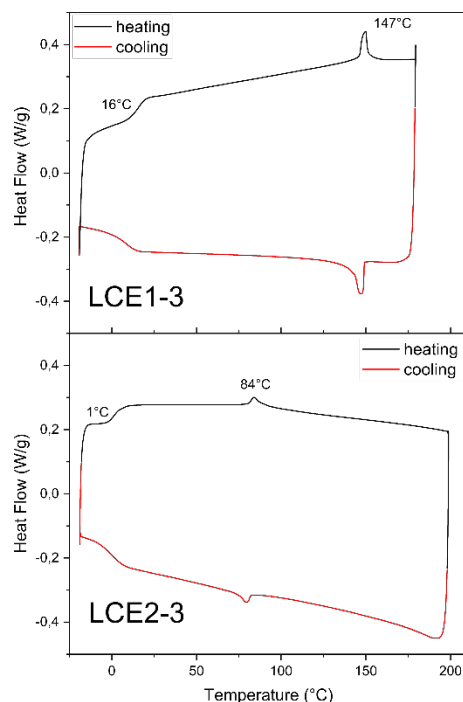


Figure 4 - DSC traces ($10\text{ }^{\circ}\text{C}/\text{min}$) corresponding to the second cycle of heating and cooling of some LCE films.

All T_g values are below room temperature with the polymer containing T2 showing the lowest value (1 °C). In this case, the contribution of the alkyne is more pronounced resulting in the highest T_g for LCE1-1 (23° C) where the ability of the mesogens to form H-bonds can influence the overall polymer plasticity. For the other two samples (LCE1-2 and LCE1-3), increasing the number of aromatic rings in the alkyne component leads to a moderate variation of T_g (from 9 °C in LCE1-2 to 16 °C in LCE1-3).

Table 2 - Thermal properties of LCE films.

Film	T_g [°C] ^a	T_{NI} [°C] ^b	ΔH_{NI} [J/g] ^c
LCE1-1	23	151	1.26
LCE1-2	9	150	0.95
LCE1-3	16	147	2.12
LCE2-3	1	84	1.3

^a Determined from the midpoint of the baseline jump in DSC traces. ^b and ^c are determined respectively from the maximum and the area of the transition peak in the DSC traces.

On the other hand, the effect of the monomer structure on the thermo-mechanical behavior is totally different as demonstrated by the dynamic-mechanical thermal analysis (DMTA). The measurements were performed in tensile mode in both parallel and perpendicular direction with respect to the director. As a typical example, Figure 5 reports the trend of dynamic storage modulus (E') and loss tangent ($\tan \delta$) as a function of temperature for the sample LCE1-1 in both directions.

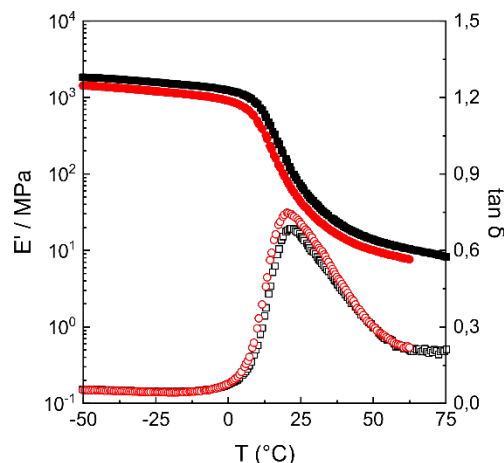


Figure 5. Trend of dynamic storage modulus E' and loss tangent $\tan \delta$ in the parallel (black symbols) and perpendicular (red symbols) directions with respect to the liquid crystalline alignment as a function of temperature for LCE1-1 sample (E' full symbols and $\tan \delta$ open symbols).

The dynamic storage modulus E' decreases with increasing temperature with a drop of two orders of magnitude corresponding to the glass transition. The E' modulus in the parallel direction (1.2 GPa at 0°C) is slightly higher than in the perpendicular one (1.0 GPa at 0°C) whereas higher $\tan \delta$ values are observed in the perpendicular direction thus indicating a more lossy behavior. Figure 6 reports E' (upper panels) and $\tan \delta$ (lower panels) in the parallel and perpendicular direction with respect to the director as a function of temperature for all the samples. LCE1-3 (red symbols) is present in both panel series and shows E' modulus and T_g higher than sample prepared with T2 molecule (two aromatic rings linked by ester groups).

As a general statement, E' in the parallel direction is always higher than in the perpendicular direction, as usually observed for different LCE formulations,³ although sometimes the difference is not very marked. The increase in the number of aromatic rings in both the main-chain and in the side-chain leads to a modulus

increase. Despite the small modulation in the thermal properties observed in the DSC, in this case, the use of different liquid crystalline alkyne is useful to modulate the mechanical properties of the samples. The formation of hydrogen bonds due to the presence of monomer A1 produces an increase in the glass transition temperature whereas lower modulus values in both directions are observed in the glassy state. Also, the damping capabilities of the materials is greatly influenced by the alkyne moieties with $\tan \delta$ value that decreased especially when the hydrogen bonding molecule A1 is present.

Beside the thermo-mechanical behavior, another important aspect to be considered in LCE characterization is their response to external stimuli. Their reversible deformation is needful for the use of these materials as actuators in many fields of research, e.g. photonics, robotics and regenerative medicine. To this aim, we performed a preliminary evaluation by analyzing the material shape-changing properties in response to temperature. The response to other stimuli could be addressed in future studies by adding dyes (for light responsive materials)²⁸ or inorganic nanoparticles and liquid metals (for electrical field response).²⁹

Different LCE stripes have been cut in a rectangular shape (with the longest dimension along the nematic director), placed on a silicon oil drop and then subjected to controlled thermal treatment. The samples have been heated up to 200 °C and then cooled down. All samples showed a contraction along the liquid crystalline alignment direction with a complete shape-recovery on cooling at room temperature (Figure 7a). The shape changing behavior is reversible for several times (we tested at least 30 heating cycles) and Figure S12 report the relative length of LCE1-3 during a complete heating and cooling cycle.

However, temperature response profiles significantly vary depending on the formulation. The more pronounced differences were shown by the materials having different LC components in the main-chain (T1 or T2). The graph in Figure 7b shows the relative length of each stripe (reported as a percentage and calculated with respect to the stripe length at room temperature) as a function of the temperature during the heating stage. For all polymers, a maximum deformation around the 40% of the original length has been observed, confirming as these materials are capable of larger deformations than acrylate-based LCEs.³⁰

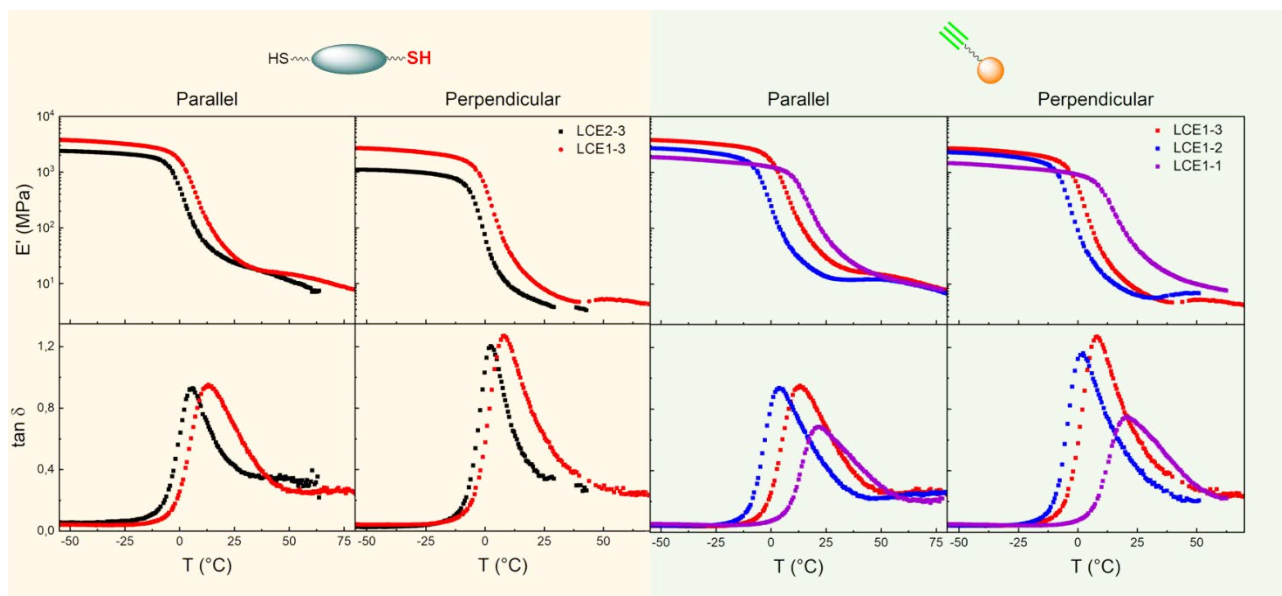


Figure 6. Trend of dynamic storage modulus E' (upper panels) and loss tangent $\tan \delta$ (lower panels) in the parallel and perpendicular directions with respect to the liquid crystalline alignment as a function of temperature for all samples

Surprisingly, in the T1 material series, variation of the architecture from “end-on” to “side-on” in the side-chain component (LCE1-2 vs LCE1-3) seems to not significantly influence the response of the polymer. This result is in contrast with the observation made for “side-chain” LCEs by acrylate polymerization.³¹ In that case, the “side-on” conformation led to an enhanced coupling in between the polymer chain and the LC units resulting in a larger deformation under stimuli.³² On the other hand, for the materials presented here, the main-chain LC component plays the major role in determining the contraction behavior. Looking at LCE1-1 sample, the insertion of the hydrogen-bonding units did not significantly change the thermal response, in agreement with the previously shown DSC analysis. Formulations containing T1 lead to a small gradual deformation during the heating up to the clearing temperature (around 150 °C for each film) while above this point, a sharp shape-change is observed up to the maximum contraction.

More interesting results were obtained with LCE2-3, showing a clearing temperature of 84 °C. The low clearing temperature of this sample leads to a different response to temperature with respect to the other formulations: when LCE2-3 reaches its maximum deformation, the thermal response of the other stripes is really small (less than 5%), thus resulting in a decouple of the environment responsiveness of LCE having different LC main-chain components.

Actuators that respond differently to the same stimulus are very appealing to create remotely controlled robots. This is of particular interest in micro robotics where the application of a stimulus/signal to a selected body part of the robot is not trivial if not even impossible.³³ Therefore, preparing devices with components made by differently responsive materials, would allow to selectively activate specific parts of the robot by a flat stimulus spread out on the whole robot.

The thermal response of the here proposed LCEs can be exploited to obtain actuators that respond selectively in different temperature ranges. A simple demonstration is shown in Figure 7c and Movie S1, where different LCE stripes have been combined in a square geometry. Heating this structure, we can observe the selective actuation of LCE1-3 and LCE2-3 components. At 90° C, LCE2-3 is already activated (reaching its maximum contraction), while the 2 stripes composed by LCE1-3 are subjected only to a small length variation. Only heating up to 180° C, we can observe the complete deformation of both the elastomers (of all the 4 sides of the square). The simple geometry, here presented as a proof-of-concepts, demonstrated the possibility to prepare more complex robotic elements able to move or to perform work in an asymmetric way when subjected at a spatially flat increase of temperature.

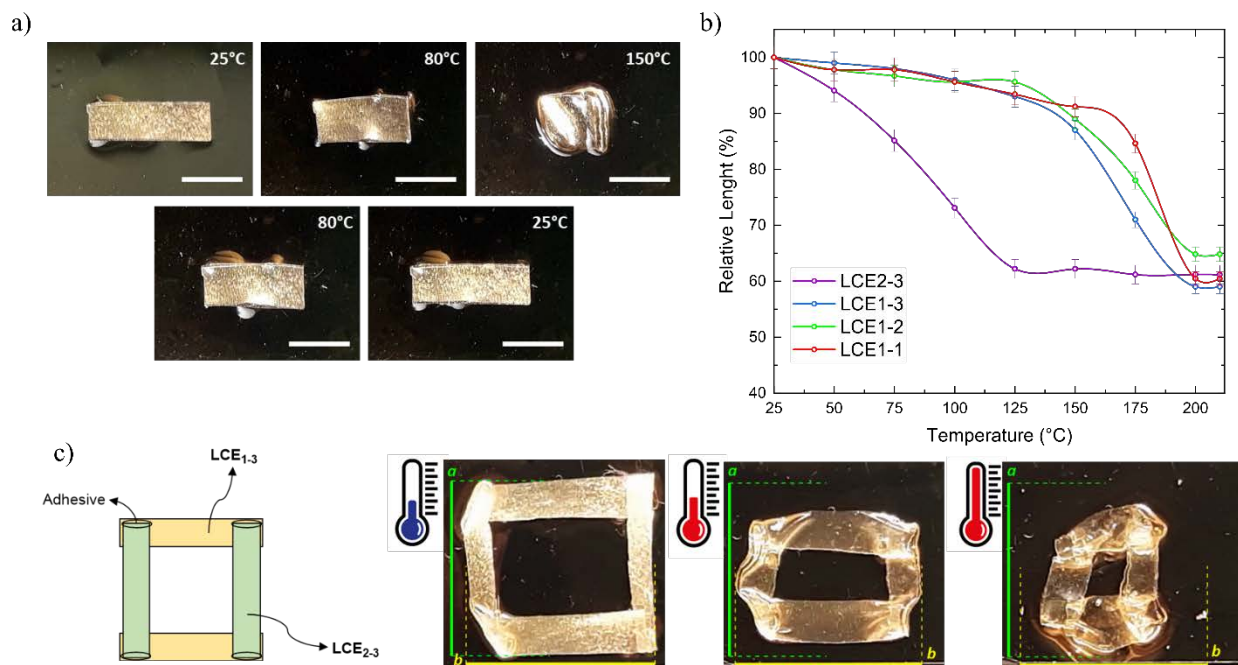


Figure 7 – Deformation of LCEs upon heating. a) Sequence of optical images reporting two stripes of LCE1-3 at different temperatures. Scale bar: 0,5 cm b) Graph of the contraction along the LC alignment direction for the LCEs at different temperatures. The % of relative length is calculated as $(L_T/L_0) \cdot 100$ where L_T is the stripe length at temperature T and L_0 is the initial length at room temperature. c) Selective deformation of different LCE stripes arranged as indicated in the left panel: optical images of a square composed by two stripes of LCE1-3 (yellow) and two stripes of LCE2-3 (green) at: 1) room temperature, 2) at 90 °C (deformation of one side- marked in green - is observed), 3) at 180 °C (deformation also of the other side- marked in yellow - is achieved).

4. CONCLUSIONS

Several Liquid Crystalline Elastomers were prepared by thiol-yne click chemistry with an unusual mixed architecture which can be tuned to selectively control the material properties. Playing with the liquid crystalline units inserted as side-chain, it is possible to modify the mechanical properties with little impact on the shape-changing behavior. Increasing the number of aromatic rings leads to an increase in the elastic modulus, while by inserting H-bonding units a significant decrease of the damping capability of the material. On the other hand, the LCEs actuation is impressively modulated thanks to modification of the main-chain LC component leading to materials that contract about 40% of their initial length in very different temperature ranges. With a difference in the clearing temperature up to 63 °C, we here demonstrated how to decouple the thermal response of the LCEs by properly choosing the dithiol monomer. The new understanding of the relationship between material architecture and composition, and the mechanical and thermo-responsive behavior, is of great use for applications in micro robotics. This preliminary assessment will be further exploited towards application as actuators, focusing on the possibility to extend this selective actuation, described here under heating, to different remote stimuli, such as light, by doping the polymer with azobenzenes or other light-switching molecules, to obtain smart asymmetrically light-controlled devices. Finally, by acting on both components, the dithiol and the alkyne monomers, would allow to try answering unsolved issues in the bio-medical field. From complex scaffolds for cell culture to high dissipative materials, the efficient modulation of elastic modulus and damping capability could be obtained leading to improved solutions. Last but not least, the novel formulations would be also suitable materials to be nanopatterned by different lithographic techniques to obtain 2D patterned surfaces or 3D deformable objects.

ASSOCIATED CONTENT

Supporting Information. The Supporting Information is available free of charge at “xxx” and includes: monomer synthetic procedures, DSC traces of monomers and polymers, POM images of monomers, FT-IR spectra of monomers and polymers, movie showing the thermal contraction of polymers.

AUTHOR INFORMATION

Corresponding Authors

* Daniele Martella e-mail: martella@lens.unifi.it

* Camilla Parmeggiani e-mail: camilla.parmeggiani@unifi.it

Author Contributions

F.L, D.M. performed the experiments, S.N. supervised the material characterization, D.M. and C.P designed the experiments, D.A. and M.L performed the mechanical characterization, all the authors wrote the manuscript.

ACKNOWLEDGMENT

Financial support from Ente Cassa di Risparmio di Firenze (grant 2017/0713 and 2020/1583) is acknowledged.

REFERENCES

- (1) Ohm, C.; Brehmer, M.; Zentel, R. Liquid Crystalline Elastomers as Actuators and Sensors. *Adv. Mater.* **2010**, *22*, 3366.
- (2) Ware, T. H.; Biggins, J. S.; Shick, A. F., Warner M.; White T. J. Localized soft elasticity in liquid crystal elastomers. *Nat. Commun.* **2016**, *7*, 10781.
- (3) Auguste, D. A.; Ward, J. W.; Hardin, J. O.; Kowalski, B. A.; Guin, T. C.; Berrigan, J. D.; White, T. J. Enabling and Localizing Omnidirectional Nonlinear Deformation in Liquid Crystalline Elastomers. *Adv. Mater.* **2018**, *30*, 1802438.
- (4) Saed, M. O.; Volpe, R. H.; Traugott, N. A.; Visvanathan, R.; Clark, N. A.; Yakacki, C. M. High strain actuation liquid crystal elastomers *via* modulation of mesophase structure. *Soft Matter* **2017**, *13*, 7537.
- (5) Shaha, R. K.; Merkel, D. R.; Anderson, M. P.; Devereaux E. J.; Patel, R. R.; Torbati, A. H.; Willett, N.; Yakacki, C. M., Frick C. P. Biocompatible liquid-crystal elastomers mimic the intervertebral disc. *J. Mech. Behav. Biomed.* **2020**, *107*, 103757.
- (6) Winkler, M.; Kaiser, A.; Krause, S.; Finkelmann, H.; Schmidt, A. M. Liquid crystal elastomers with magnetic actuation. *Macromol. Symp.* **2010**, *291*, 186.
- (7) Agrawal, A.; Chen, H.; Kim, H.; Zhu, B.; Adetiba, O.; Miranda, A.; Chipara, A. C.; Ajayan, P. M.; Jacot, J. G.; Verduzco, R. Electromechanically responsive liquid crystal elastomer nanocomposites for active cell culture. *ACS Macro Lett.* **2016**, *5*, 1386.
- (8) Ikeda, T.; Mamiya, J.; Yu Y. Photomechanics of liquid-crystalline elastomers and other polymers. *Angew. Chem. Int. Ed.* **2007**, *46*, 506.
- (9) Kowalski, B. A.; Guin, T. C.; Auguste, A. D.; Godman, N. P.; White, T. J. Pixelated polymers: directed self-assembly of liquid crystalline polymer networks. *ACS Macro Lett.* **2017**, *6*, 436.
- (10) Li, M-H.; Keller, P. Artificial muscles based on liquid crystal elastomers. *Phil. Trans. R. Soc. A.* **2006**, *364*, 2763.
- (11) Ferrantini, C.; Pioner, J. M.; Martella, D.; Coppini, R.; Piroddi, N.; Paoli, P.; Calamai, M.; Pavone, F. S.; Wiersma, D. S.; Tesi, C.; Cerbai, E.; Poggesi, C.; Sacconi, L.; Parmeggiani, C. Development of Light-Responsive Liquid Crystalline Elastomers to Assist Cardiac Contraction. *Circ Res.* **2019**, *124*, e44.

- (12) Martella, D.; Parmeggiani, C. Advances in Cell Scaffolds for Tissue Engineering: The Value of Liquid Crystalline Elastomers. *Chem. Eur. J.* **2018**, *24*, 12206-12220.
- (13) Liu, D.; Broer, D. J. Liquid Crystal Polymer Networks: Preparation, Properties, and Applications of Films with Patterned Molecular Alignment. *Langmuir* **2014**, *30*, 13499.
- (14) Wareab, T. H.; White, T. J. Programmed liquid crystal elastomers with tunable actuation strain. *Polym. Chem.* **2015**, *6*, 4835.
- (15) Yakacki, C. M.; Saed, M.; Nair, D. P.; Gong, T.; Reed, S. M.; Bowman, C. N. Tailorable and programmable liquid-crystalline elastomers using a two-stage thiol-acrylate reaction. *RSC Adv.* **2015**, *5*, 18997.
- (16) Saed, M. O.; Ambulo, C. P.; Kim, H.; De, R.; Raval, V.; Searles K.; Siddiqui, D. A.; Cue, J. M. O.; Stefan, M. C.; Shankar, R. M.; Ware, T. H. Molecularly-Engineered, 4D-Printed Liquid Crystal Elastomer Actuators. *Adv. Funct. Mater.* **2019**, *29*, 1806412.
- (17) Godman, N. P.; Kowalski, B. A.; Auguste, A. D.; Koerner, H.; White, T. J. Synthesis of elastomeric liquid crystalline polymer networks via chain transfer. *ACS Macro Lett.* **2017**, *6*, 1290.
- (18) De Bellis, I.; Ni, B.; Martella, D.; Parmeggiani, C.; Keller, P.; Wiersma D. S.; Li, M-H.; Nocentini, S. Color Modulation in *Morpho* Butterfly Wings Using Liquid Crystalline Elastomers. *Adv. Intell. Syst.* **2020**, *2*, 2000035.
- (19) Martella, D.; Parmeggiani, C.; Wiersma, D. S.; Piñol, M.; Oriol, L. The first thiol-yne click chemistry approach for the preparation of liquid crystalline elastomers. *J. Mater. Chem C*, **2015**, *3*, 9003.
- (20) Lowe, A. B.; Hoyleb, C. E.; Bowman; C. N. Thiol-yne click chemistry: A powerful and versatile methodology for materials synthesis. *J. Mater. Chem.* **2010**, *20*, 4745.
- (21) Lowe, A. B. Thiol-yne 'click'/coupling chemistry and recent applications in polymer and materials synthesis and modification. *Polymer* **2014**, *55*, 5517.
- (22) Nocentini, S.; Martella, D.; Parmeggiani, C.; Wiersma, D.S. Photoresist Design for Elastomeric Light Tunable Photonic Devices. *Materials* **2016**, *9*, 525.
- (23) Yang, H.; Buguin, A.; Taulemesse, J-M.; Kaneko, K.; Méry, S.; Bergeret, A.; Keller, P. Micron-Sized Main-Chain Liquid Crystalline Elastomer Actuators with Ultralarge Amplitude Contractions. *J. Mater. Chem.* **2009**, *131*, 1500.
- (24) Zentel, R.; Brehmer, M. Combined LC main chain/side chain polymers. *Acta polymerica*, **1996**, *47*, 141.
- (25) Pal, S. K.; Raghunathan, V. A.; Kumar; S. Phase transitions in novel disulphide-bridged alkoxyphenyl dimers. *Liq. Cryst.* **2007**, *34*, 135.
- (26) Martella, D.; Nocentini, S.; Antonioli, D.; Laus, M.; Wiersma, D.S.; Parmeggiani, C. Opposite Self-Folding Behavior of Polymeric Photoresponsive Actuators Enabled by a Molecular Approach. *Polymers* **2019**, *11*, 1644.
- (27) Nocentini, S.; Martella, D.; Parmeggiani, C.; Wiersma, D.S. 3D Printed Photoresponsive Materials for Photonics *Adv. Opt. Mater.* **2019**, *7*, 1900156.
- (28) Martella, D.; Nocentini, S.; Micheletti, F.; Wiersma, D.S.; Parmeggiani, C. Polarization-dependent deformation in light responsive polymers doped by dichroic dyes. *Soft Matter*, **2019**, *15*, 1312.
- (29) Ford, M. J.; Ambulo, C. P.; Kent, T. A.; Markvicka, E. J.; Pan, C.; Malen, J.; Ware, T. H.; Majidi, C. A multifunctional shape-morphing elastomer with liquid metal inclusions *PNAS* **2019**, *116*, 21438.
- (30) Martella, D.; Antonioli, D.; Nocentini, S.; Wiersma, D.S.; Galli, G.; Laus, M.; Parmeggiani, C. Light activated non-reciprocal motion in liquid crystalline networks by designed microactuator architecture. *RSC Adv.* **2017**, *7*, 19940.
- (31) Nocentini, S.; Martella, D.; Wiersma, D.S.; Parmeggiani, C. Beam steering by liquid crystal elastomer fibres. *Soft Matter* **2017**, *13*, 8590.
- (32) Thomsen, D. L.; Keller, P.; Naciri, J.; Pink, R.; Jeon, H.; Shenoy, D.; Ratna, B. R. Liquid Crystal Elastomers with Mechanical Properties of a Muscle. *Macromolecules* **2001**, *34*, 5868.
- (33) Nocentini, S.; Parmeggiani, C.; Martella, D.; Wiersma, D.S. Optically Driven Soft Micro Robotics. *Adv. Opt. Mater.* **2018**, *6*, 1800207.

